



HAL
open science

A Bloch wave reduction scheme for ultrafast band diagram and dynamic response computation in periodic structures

Régis F Boukadia, Christophe Droz, Mohamed N Ichchou, Wim Desmet

► **To cite this version:**

Régis F Boukadia, Christophe Droz, Mohamed N Ichchou, Wim Desmet. A Bloch wave reduction scheme for ultrafast band diagram and dynamic response computation in periodic structures. *Finite Elements in Analysis and Design*, 2018, 148, pp.1-12. 10.1016/j.finel.2018.05.007 . hal-03373014

HAL Id: hal-03373014

<https://hal.science/hal-03373014>

Submitted on 11 Oct 2021

HAL is a multi-disciplinary open access archive for the deposit and dissemination of scientific research documents, whether they are published or not. The documents may come from teaching and research institutions in France or abroad, or from public or private research centers.

L'archive ouverte pluridisciplinaire **HAL**, est destinée au dépôt et à la diffusion de documents scientifiques de niveau recherche, publiés ou non, émanant des établissements d'enseignement et de recherche français ou étrangers, des laboratoires publics ou privés.

A Bloch wave reduction scheme for ultrafast band diagram and dynamic response computation in periodic structures

Régis F. Boukadia^{a,b,*}, Christophe Droz^{b,*}, Mohamed N. Ichchou^a, Wim Desmet^b

^aÉcole Centrale de Lyon, 36 Avenue Guy de Collongue, 69134 Écully Cedex, France

^bKU Leuven, Department of Mechanical Engineering, Division PMA - Member of Flanders Make, Celestijnenlaan 300 - box 2420, Leuven, Belgium

Abstract

A variety of Reduced-Order Modelling (ROM) techniques have been developed for the Wave/Finite Element (WFE) Framework. However most of these techniques are not compatible with dynamic response computation or frequency-dependent problems. This paper introduces a new reduction strategy for the WFE method, enabling the computation of both the forced response and the complex dispersion curves of periodic structures modelled using large-sized finite element (FE) models. The method exploits the duality between Inverse and Direct Bloch formulations to build a reduced solution subspace, accounting for both propagating and evanescent behaviours, while ensuring high reduction factors. This reduction strategy therefore enables the resolution of a wider range of problems, including near/far field response computation in finite waveguides subjected to dynamic loadings, or vibroacoustic transmission/reflection problems. First, the method is used to compute dispersion curves and forced response in a duct. Then a large bi-stiffened structure is studied to evaluate the method's performances. The high frequency resolution provided by the proposed ROM allows us to explore a variety of propagation and guided resonances localization effects, hardly accessible otherwise. Furthermore, the considerable reduction factors enable fast wave dispersion analyses in large-scaled periodic structures, complex phononic crystals designs or locally resonant metamaterials.

Keywords: Wave Finite Element, Bloch theorem, Model reduction, Forced response, Evanescent waves, Periodic structures

Contents

1	Introduction	2
2	Review of the WFEM framework	4
2.1	Inverse and direct approach pros and cons	4
2.2	Modal-based, wave-based and hybrid reduction methods	6

*Co-first authors. These authors contributed equally to the article.

3	Proposed reduction scheme	7
3.1	Computation of the cut-on frequencies for $ \lambda = 1 $	8
3.2	Computation of the direct solution at ω_{\max}	8
3.3	Computation of the inverse solutions and k-space sampling	8
3.4	Singular Value Decomposition and wave basis truncation	9
4	Validation 1: application to a hollow beam	10
4.1	Presentation of the model	11
4.2	Performance of the method for dispersion analysis	11
4.3	Performance of the method on a forced response framework	13
5	Validation 2: application to a stiffened plate	15
5.1	Description of the stiffened structure	16
5.2	Results and discussion of propagative behaviours in stiffened plates	16
5.3	Waveguiding along stiffeners	19
6	Conclusion	20

1. Introduction

An extensive research effort has been devoted to understand and analyse wave propagation in periodic structures, meta-materials and a broad range of lightweight structures over the past decade. Their periodicity allows the computation of local wave dispersion characteristics such as stop-bands, local resonances, diffusion and spatial attenuation properties. This knowledge can then be used for the design and optimization of a broad range of engineered media with desirable dynamic behaviours (see [1, 2, 3, 4]). Various methods were developed to predict wave dispersion characteristics in complex 1D or 2D periodic structures: homogenization techniques were proposed in [5] to compute high-frequency dispersion characteristics in phononic waveguides. One can also cite the work Boutin et al. [6] on equivalent models for porous waveguides with embedded Helmholtz resonators. Multi-scale techniques were also developed [7, 8] to model heterogeneous or periodic structures using limited macroscopic information. Recently, the wave finite element method (WFEM) based on Bloch theorem, has been the subject of high interest (see Sec. 2 for a detailed discussion). It has been used to study wave propagation and conduct vibroacoustic analyses in a wide range of continuous or periodic structures, as it exploits standard FE packages to model the waveguide’s unit-cell. One can cite applications of the WFEM to structures such as sandwich panels involving different core topologies [9, 10], poroelastic media [11] or piezoelectric elements [2]. It was recently applied to perform fast design of periodic topologies with enhanced acoustic performances by computing local acoustic radiation [12] or transmission [13, 14] problems in a variety periodic structures.

In order to further enable the development of novel acoustic or elastic meta-structures with optimized structural configurations, considerable challenges are still to be faced in terms of numerical methodologies. Indeed, computing the broadband dispersion diagram of complex periodic waveguides requires to solve numerous large, often ill-conditioned (see Waki et al. [15]) eigenvalue problems, whose size is related to the FE model used to describe the waveguide's unit-cell. Remarkable achievements have been achieved on reduced-order modelling (ROM) strategies for wave-based methods and particularly for the wave finite element framework. Those are driven by the need to use refined unit-cell's finite element model when the wavelength are small compared with the unit-cell's length. Reduction schemes are also crucial to enable fast design of complex structures (e.g. to create locally resonant behaviours, see [16] for example) or to implement topology optimization algorithms (see Kook and Jensen [17]). Various ROM strategies have been developed for the WFEM, enabling fast wave analyses at different levels:

- A reduction strategy for computing the forced response for 1D waveguides was developed by Mencik [18, 19], along with significant improvements on the computational efficiency and conditioning of the matrices. This yields a better exploitation of the computed wave solutions to retrieve the harmonic response of a finite waveguide.
- Condensation techniques have been introduced in the WFE framework (see [20]) to reduce the computational effort associated with the dynamic condensation of the inner degrees of freedom (DOF) of the unit-cells.
- Finally, Droz et al. [21, 22] developed an interface reduction technique to replace also the periodic edge DOF by a reduced number of propagating Bloch waves. Combined with modal condensation techniques, this method provides the dispersion curves in complex periodic structures with up to 99% reduction of the computational effort.

However, it is emphasized that only propagating and slightly decaying wave solutions can be derived from the wave expansion strategy mentioned above. Nonetheless, evanescent waves are crucial to describe the local dynamics at a waveguide's edges, or close to structural singularities (e.g. a coupling element, a point force excitation). Therefore it is obvious that none of the above mentioned ROM strategies allows both an ultrafast computation of the dispersion curves and a further exploitation for coupling or forced response computation. This work therefore aims at the development of a reduced formulation of the dispersion problem allowing the computation of both propagating and evanescent waves. This will enable a further use of the obtained solutions to predict the response to complex load cases or to perform fast diffusion analyses through finely meshed sub-structures.

In this paper a model order reduction strategy is developed for the wave/finite element framework, based on singular value decomposition of a discretized wave solution subset. The paper is organized into 6 sections including this introduction. The background on WFEM is reviewed in Sec. 2 and some numerical issues related to Bloch wave analysis are discussed. In Sec. 3 the proposed model order reduction scheme is described for the fast computation of propagating and evanescent waves based on singular value decomposition. In Sec. 4, the reduction scheme is

applied to a hollow beam, which is a typical case of continuous waveguide exhibiting multimodal behaviour when subjected to a point force excitation in the medium frequency range. The reduced model is used to compute wave dispersion characteristics and the approximation error. Then, the forced response is computed in the finite structure, to highlight the method's performances in the forced WFEM framework. In Sec. 5, the performances of the method are challenged for a full-scaled stiffened plate with an large unit-cell's FE model. The vibroacoustic behaviour of this periodic structure is commonly studied though wave-based approaches and requires the combination of the WFEM with a CMS technique. The proposed reduction scheme is therefore applied to explore veering, locking and stopband effects produced by the stiffeners, with a frequency resolution that could not be achieved without ROM strategy. Conclusion are eventually drawn in Sec. 6.

2. Review of the WFEM framework

The WFEM framework correspond to the application of Floquet-Bloch conditions on FE models of unit cells to compute the properties of waves in a periodic media. First, a finite element model is obtained using an FE package, the mesh of the unit cell should respect periodicity conditions ensuring that primal assembly of the right and left interfaces of the unit cell is possible. Then, the degrees of freedom of the unit cell are separated in three groups: q_L the degrees of freedom of the left interface, q_I , the internal degrees of freedom of the unit cell and q_R the degrees of freedom of the right interface. Finally, Bloch periodicity conditions are applied on the unit cell namely : $q_R = \lambda q_L$ and $f_R = -\lambda f_L$. f_L and f_R representing the efforts on the right and left interface and λ being the Floquet-Bloch propagation constant.

2.1. Inverse and direct approach pros and cons

Initially developed by Mead [23], the inverse approach consist in fixing the propagative constant λ of a periodic structure and compute the unknown frequencies ω_i , solutions of the following eigenvalue problem:

$$(\mathbb{K}(\lambda) + j\omega_i\mathbb{C}(\lambda) - \omega_i^2\mathbb{M}(\lambda))\Phi_i = \mathbf{0} \quad (1)$$

where the matrices \mathbb{K} , \mathbb{C} and \mathbb{M} are respectively the stiffness, damping and mass operators of the waveguide's periodic unit-cell obtained by forcing the value of the propagation constant (see equation (6) for explicit formulation). It is therefore emphasized that viscous and hysteretic damping models are handled by this formulation, although more complex damping models would require the resolution of non-linear eigenvalue problems:

$$(\mathbf{K}(\omega_i, \lambda) - \omega_i^2\mathbb{M}(\lambda))\Phi_i = \mathbf{0} \quad (2)$$

The formulation in Eq.1 has the advantage that the matrices $\mathbb{K}(\lambda)$, $\mathbb{C}(\lambda)$ and $\mathbb{M}(\lambda)$ are symmetric positive whenever the propagating constant λ is equal to 1 or -1 (the solutions ω_i are therefore corresponding to the so-called *cut-on* frequencies). Additionally, these matrices are self-adjoint for all the complex propagating constants located in

the unit circle. This means the eigenvalue problem is well-conditioned, especially when no damping is present. The eigenvalues ω_i and eigenvectors Φ_i pairs obtained by this method exhibit higher accuracy and reliability, while iterative solvers can be used to limit the computation to a solution subset of interest. This inverse method however, has a number of drawbacks:

- a- The size of the eigenvalue problem is $(n + m)$ where n is the number of DOF on the section and m is the number of DOF on the inner part of the structure.
- b- Since frequency is the unknown of eigenvalue problem Eq.(1), the use of frequency-dependent material properties (such as damping) is not straightforward. As a consequence, the prediction of non-propagating waves in dissipative materials is limited.
- c- The method is not compatible with frequency-based approaches such as the forced/coupling formulations derived from the WFEM outputs (see Mencik and al. [18])

As a consequence of these issues, the direct approach was later developed [24]. The direct approach assumes a known frequency and uses dynamic condensation of the m inner DOF of the structure to reduce the size of the spectral problem from $(n + m)$ to n . An $(n \times n)$ eigenvalue problem is then solved with the propagating constants as unknowns. This eigenvalue problem can take the following among many forms([25, 26]):

$$\left(\frac{1}{\lambda}\tilde{D}_{RL} + (\tilde{D}_{RR} + \tilde{D}_{LL}) + \lambda\tilde{D}_{LR}\right)q_L = 0 \quad (3)$$

where the subscripts ${}_L$ and ${}_R$ denote the left- and right-sided DOF of the condensed dynamic stiffness matrix \tilde{D} of the periodic unit-cell.

This direct approach has the advantage of giving all the propagating constants at a given frequency and is compatible with frequency-dependent damping models. However, these advantages are counterbalanced by a number of numerical issues [27]. Indeed, the spectral problem can only be solved once put on the following form:

$$(\tilde{D}_{RL} + \lambda(\tilde{D}_{RR} + \tilde{D}_{LL}) + \lambda^2\tilde{D}_{LR})q_L = 0 \quad (4)$$

This quadratic eigenvalue problem is equivalent to Eq.(3) **if and only if** the matrix \mathbf{D}_{RL} (or \mathbf{D}_{LR}) can be inverted, which is not the case in practice. This leads to pairs of 0 and ∞ eigenvalues corresponding to eigenvectors located in the kernels of \mathbf{D}_{RL} and \mathbf{D}_{LR} . These solutions must be filtered out since they have no physical meaning and strongly degrade the condition of the eigenvalue problem. It should be noted that bad conditioning can arise even when all the matrices are non-degenerate: this can be due to the presence of strongly evanescent waves and the limitations of machine precision. A better formulation for the computation of eigenvalues was developed by Zhong et al. [28]. It has the advantage of improving the condition number of the eigenvalue problem by gathering the pairs of the symplectic eigenvalue problem into a eigenspace of dimension 2 and associating strongly evanescent waves with a strictly 0 eigenvalue instead of $(0, \infty)$ pairs.

2.2. Modal-based, wave-based and hybrid reduction methods

In order to increase the computational effectiveness of the method, model order reduction strategies have been developed in the WFEM framework: Zhou et al. [20] developed a model order reduction strategy based on the Craig-Bampton reduction of the inner DOF of the structure. The method has been shown to yield good results when a number of $\tilde{m} \ll m$ modes of frequencies up to three times the maximum frequency of study are retained. When used in conjunction to the inverse approach, the method results in a direct reduction of the size of the eigenvalue problem from $n + m$ to $n + \tilde{m}$. When used in conjunction to the direct approach, the size of the eigenvalue problem (n) is not reduced but the inversion of the sub-matrix \mathbf{D}_{Π} is highly facilitated.

For the direct approach, Droz et al. [21] developed a wave-based reduction strategy to compute propagating solutions of waveguides involving complex cross-sectional FE model. The eigenvalue problem is then reduced from n cross-sectional DOF to a reduced number $\tilde{n} \ll n$ of propagating wave contributions, hence providing considerable reduction of the computational costs associated with wave dispersion analyses. The reduced wave basis is formed using propagating eigenvectors filtered from a limited number of full solutions sampled on cut-on frequencies. Gram-Schmidt Ortho-normalization is then used to create a projection matrix containing selected wave-shapes. Although this method can be used to perform a fast computation of propagating dispersion curves, it suffers from the following limitations:

- a- Depending on frequency sampling, Gram-Schmidt algorithm can produce redundant projection basis and yield numerical noise, as well as an unnecessary large reduced basis. Its reduction hence requires an additional truncation criteria which may result in a lack of robustness of the method, especially when a large number of cut-on frequencies are located in the bandwidth of interest.
- b- A variety of frequency-dependent phenomena can occur far from selected frequency samples, or without the appearance of a cut-on frequency: one can cite wave conversions, localizations or other periodic effects. In such cases, the reduced basis is not expected to allow accurate computation of the wave dispersion characteristics.
- c- Finally, the method was created only aiming at predicting propagating dispersion curves. Since evanescent waves are missing in the reduced model, the use of diffusion or forced computation framework is not available. Such a reduction method, compatible with the forced response and wave diffusion framework is still missing in the literature.

In order to address these issues, a new reduction method is proposed hereby, combining the advantages of inverse method (i.e. iterative solver and well-conditioned matrices) with a direct WFEM formulation able to tackle frequency-dependent FE models. In addition to being more accurate and robust, this reduction strategy provides both propagating and evanescent solutions and is compatible with wave-based framework for forced response computation.

3. Proposed reduction scheme

The proposed reduction method combines the Craig-Bampton reduction method with a wave based reduction (see also [22]). First, the Craig-Bampton reduction is applied resulting in a reduction of the number of inner DOF from m to \tilde{m} . The component modes of the periodic unit-cell are kept up to $4 \times f_{max}$, to ensure accurate description of the inner motions for evanescent waves. Reduced matrices are denoted \mathbf{K} , \mathbf{C} and \mathbf{M} while dynamic condensation of the inner DOF q_I is applied in the direct method, so that the dynamic stiffness matrix at the frequency ω is denoted $\tilde{\mathbf{D}}$. The idea is to build a projection basis for the interface DOF q_L and q_R , able to capture the propagative waves as well as the least evanescent waves that have significant contributions to the dynamical response of the structure close to its boundaries. To build this reduced basis from an accurate and computationally efficient way, it is preferable to use wave shapes corresponding propagative solutions obtained mainly through the use of the inverse method. The main advantage of using the inverse method is that eigenvalues and eigenvectors are well conditioned for a given wavenumber k and correspond to eigen-frequencies allowing frequency-based truncations of the model similar to classical mode-based ROM strategies. Preliminary information about the $k - space$ topology is necessary to define a judicious and robust sampling strategy. It is therefore needed to evaluate: (1) the number of propagating waves appearing in the bandwidth of interest and their cut-on frequencies ; (2) if waves reach aliasing, what is their cut-off frequencies (e.g. in case of bandgap or Bragg aliasing) ; and (3) what is the wavenumber's value and the maximal frequency of interest. An illustration is shown in Fig.1 to describe the combination of inverse and direct methods for retrieving these solutions.

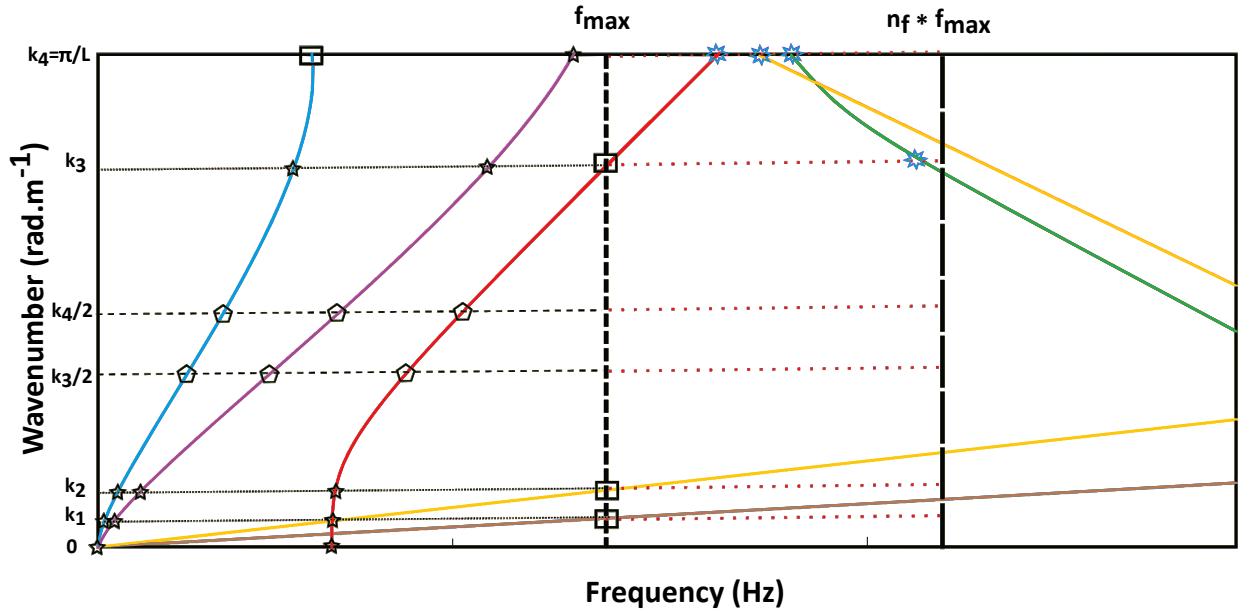


Figure 1: Illustration of the $k - space$ sampling strategy.

The sampling strategy is to determine values of k for which the inverse approach will be used. The sampling set

is initialized with $k_0 = 0$. In the first step of the method the direct approach is used at a single frequency: f_{max} to retrieve the propagating values of k . These values are depicted by the square markers on the vertical dashed line at f_{max} . The three values k_1, k_2 and k_3 are added to the sampling pool. Then the inverse approach is used with $k = \frac{\pi}{L}$ to determine if aliasing is reached before f_{max} . Since this is the case (square marker on the horizontal line), the value at $k_4 = \frac{\pi}{L}$ is also added to the initial sampling pool. The parameter n_k is then introduced to refined the wavenumber sampling. It ensures that each wave is sampled at least n_k times and no effect of wave conversion or veering is missed. Therefore, using $n_k = 2$ yields the following additional k -values: $\frac{k_1}{2}, \frac{k_2}{2}, \frac{k_3}{2}, \frac{k_4}{2}$ (c.f. horizontal dashed lines in Fig. 1). The inverse approach is then used at each k -sample and the eigenfrequencies are kept below $n_f \times f_{max}$. This frequency parameter allows a projection basis enrichment able to account for some non-propagative waves, hence to increase the performance of the method in the forced response framework. These solutions are shown in Fig.1 for the main k -samples (star markers), refined samples (pentagon markers, depending on n_k) and first step solution (square markers).

3.1. Computation of the cut-on frequencies for $|\lambda| = 1$

First, the inverse approach is used with λ equal to 1 and -1 to retrieve the cut-on frequencies by solving the following eigenvalue problem:

$$(\mathbf{K}(\lambda) + j\omega_i\mathbf{C}(\lambda) - \omega_i^2\mathbf{M}(\lambda))\Phi_i = \mathbf{0} \quad (5)$$

where the matrix operator $\lambda \longrightarrow X(\lambda)$ is defined by:

$$X(\lambda) = \begin{pmatrix} I_n & 0 & \frac{1}{\lambda}I_n \\ 0 & I_m & 0 \end{pmatrix} \times \begin{pmatrix} X_{LL} & X_{LI} & X_{LR} \\ X_{IL} & X_{II} & X_{IR} \\ X_{RL} & X_{RI} & X_{RR} \end{pmatrix} \times \begin{pmatrix} I_n & 0 \\ 0 & I_m \\ \lambda I_n & 0 \end{pmatrix} \quad (6)$$

The obtained cut-on and cut-off frequencies and associated wave-shapes provide valuable information about band-gaps, Bragg aliasing and possible appearance of new propagating waves.

3.2. Computation of the direct solution at ω_{max}

A direct approach is then used to determine the constants of propagation and wave-shapes of waves that did not reach aliasing on the frequency range. A single resolution of Eq.(3) is therefore needed at the frequency ω_{max} .

$$\left(\frac{1}{\lambda}\tilde{\mathbf{D}}_{RL} + (\tilde{\mathbf{D}}_{RR} + \tilde{\mathbf{D}}_{LL}) + \lambda\tilde{\mathbf{D}}_{LR}\right)\mathbf{q}_L = \mathbf{0} \quad (7)$$

3.3. Computation of the inverse solutions and k -space sampling

It was recently shown [9] shown that wave frequency-conversions can happen and may result in drastic variations of the wave-shapes (i.e. eigenvectors) on a same given branch of the dispersion diagram. In order to capture those changes, the k -space is sampled based on the wavenumber solutions computed above, according to the following procedure. Denoting $k_p^{(max)}$ the real part of the wavenumber of the p -th propagating wave at ω_{max} , a number n_k of

samples is defined for this wave so that the sampling value $\{k_p^{(\max)}\}$ becomes $\left\{\frac{\alpha k_p^{(\max)}}{n_k}\right\}_{\alpha=\{-n_k, \dots, n_k\}}$. As a consequence, the wavenumber values used to sample the k-space are defined as:

$$\text{Samp}_k = \bigcup_p \left\{ \frac{\alpha k_p^{(\max)}}{n_k} ; \alpha = \{-n_k, \dots, n_k\} \right\}_p \quad (8)$$

An iterative Arnoldi Algorithm is used to solve the inverse problem at each wavenumber sample in Samp_k and retrieve propagating and evanescent wave-shapes up to the maximal frequency $n_f \times f_{\max}$. The parameter n_f allows to incorporate the least evanescent wave modes by sampling them once they become propagative. Given that the inverse approach is a form of modal analysis, this can be directly compared to mode based model order reduction methods where it is recommended to take modes up to n times the maximal frequency of interest as these modes still contribute to the response of the structure. The main difference, here, is the multiscale nature of the problem. If one is only interested in the response in the far field then n_f can be chosen equal to 1 without any loss of accuracy.

3.4. Singular Value Decomposition and wave basis truncation

The large collection of wave-shapes obtained from the previous steps cannot be immediately used to build a reduced projection basis. The first reason is linked to the nature of the eigenvectors used to build the reduced basis. Indeed, both inverse and direct approaches result in complex propagation constants and eigenvectors, which would produce a non-Hermitian projection basis. Although a complex projection basis is usually acceptable compared with an unstructured complex matrix, it would still degrade the computing performances of the reduced model. Therefore a separation of the real and imaginary parts of retained vectors is achieved: $\{\Psi_i\} \rightarrow \{\Re(\Psi_i) ; \Im(\Psi_i)\}$, hence doubling the size of the projection vectors collection. The second reason is related to the important redundancies within the vectors collection, meaning that the obtained projection matrix would not be of maximal rank. Such projection would result in numerical instabilities in the reduced model. To address this issue, a singular value decomposition (SVD) of the normalized vector collection Ψ_{Coll} is performed, leading to the derivation of the three matrices:

$$\Psi_{\text{Coll}} = \mathbf{U}\mathbf{\Sigma}\mathbf{V}^T \quad (9)$$

where \mathbf{U} is a $(m \times m)$ normal matrix, \mathbf{V} is a $(n \times n)$ normal matrix and $\mathbf{\Sigma}$ is a $(m \times n)$ matrix with non-negative real numbers on the diagonal and zeros outside of the diagonal.

The final wave basis projection matrix P_{LR} is built by gathering the columns of the matrix \mathbf{U} corresponding to non-null diagonal entries of $\mathbf{\Sigma}$. Note that when large values are chosen for n_f and n_k , it is possible to only keep the columns associated with the largest singular values. One of the main questions being where should the SVD be truncated, two methods are employed. Computing the effective rank [29] of the vector collection provides an estimate of the minimal number of vectors required to ensure representativeness of the projection matrix. The singular values σ_i distribution of the vector collection can be normalized by:

$$p_i = \frac{\sigma_i}{\sum_{k=1}^n \sigma_k}, \quad (10)$$

which allows computation of its entropy H :

$$H(p_1, \dots, p_n) = \sum_{i=1}^n -p_i \log(p_i) \quad (11)$$

Therefore, the effective rank of the collection of vectors can be defined as:

$$erank = \exp(H(p_1, \dots, p_n)) \quad (12)$$

The value $erank$ is the minimal number of singular values to be retained to obtain an acceptable projection basis. Note that although this criteria can be used as a default value to obtain a minimal size for the projection basis, it does not always guarantee a high quality of the reduced model. In order to evaluate the number i of first singular vectors of Ψ_{Coll} to be retained, that ensures the quality of the approximation is above an order ϵ , the following criteria is proposed to control the quality of the reduced basis:

$$\epsilon < \frac{\sum_{k=i+1}^n \sigma_k}{\sum_{k=1}^n \sigma_k} \quad (13)$$

In practice, a value of ϵ between 10^{-3} and 10^{-5} is recommended. Once the reduced wave basis P_{LR} has been obtained, the final projection basis P is formed defining the relationship between the degrees of freedom of the full and reduced models :

$$\begin{bmatrix} q_L \\ q_I \\ q_R \end{bmatrix} = \begin{bmatrix} P_{LR} & 0 & 0 \\ 0 & I & 0 \\ 0 & 0 & P_{LR} \end{bmatrix} \begin{bmatrix} \tilde{q}_L \\ q_I \\ \tilde{q}_R \end{bmatrix} \quad (14)$$

The reduced mass stiffness, and damping operators are obtained using a Rayleigh-Ritz projection on the initial matrices :

$$X_{red} = P^T X P \quad (15)$$

Where X stands for the mass stiffness, damping or dynamic stiffness matrix of the model. To obtain the dispersion characteristics of the periodic medium, the eigenvalue problems to be solved are still those of equation (3) and (1) using the reduced matrices and coordinates instead of the original ones. Therefore the model order reduction scheme proposed is directly compatible with any implementation of the WFEM.

4. Validation 1: application to a hollow beam

In this section an application example is shown to evaluate the performances of the proposed method. The reduced formulation is therefore applied to compute dispersion curves and forced response of a hollow beam. A comparison is proposed with the standard WFEM formulation, to provide discussion about computational costs and accuracy of the reduced model.

4.1. Presentation of the model

The proposed reduction scheme is tested on a rectangular hollow beam of total length: $l=12$ m, height $h=10$ cm, width $w=40$ cm, wall thickness $e=2$ mm. The beam is made of an homogeneous material of Young Modulus $E=200$ GPa, Poisson ratio $\nu=0.3$ and density $\rho=7800$ kg.m⁻³. The periodic unit-cell is described in Figure 4.1. A number of 48 elements are used in the Z-direction (height) and 12 are used in the Y-direction (width), for a total of 1440 DOF in the unit-cell.

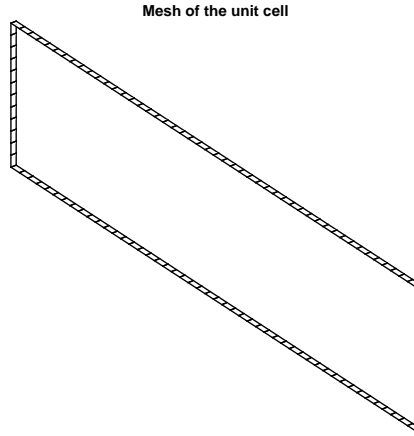


Figure 2: FEM of the hollow beam. The unit-cell is modelled on ANSYS using linear SHELL181 elements with mid-plane offset of length $l_e=4$ mm along the beam's length (X-direction).

4.2. Performance of the method for dispersion analysis

The dispersion curves of propagating waves, computed using reduced and standard WFEM, are shown in Figure 3 in the frequency range [0 - 500 Hz], while an hysteretic damping of $\eta=0.001$ is introduced in the structure. The damping η is defined as the ratio of the imaginary part over the real part of the Young Modulus. Nine propagating waves can be observed, which are subjected to various veering and frequency-conversion effects, especially around 100 Hz, where a significant increase of the wavenumbers can be observed for the two flexural modes.

With a value of $n_f=1$ and $n_k=3$, a perfect agreement can be observed between full and reduced solutions, while the total computation time for 200 frequency samples is divided by 132. As shown in table 1 the reduced model enables a considerable reduction of the computation time per frequency (1/1444), while the reduction process itself takes only 38 sec, which is comparable to the resolution of a single frequency (28 sec per frequency). This means that the frequency sampling can be considerably refined with negligible additional CPU effort.

In order to examine accuracy of the reduced model, the error is shown in Figure 4. The error produced on the approximated wavenumber k_{red} is evaluated using the values obtained for the original model k_{full} by:

$$\epsilon = \left| \frac{k_{full} - k_{red}}{k_{full}} \right| \quad (16)$$

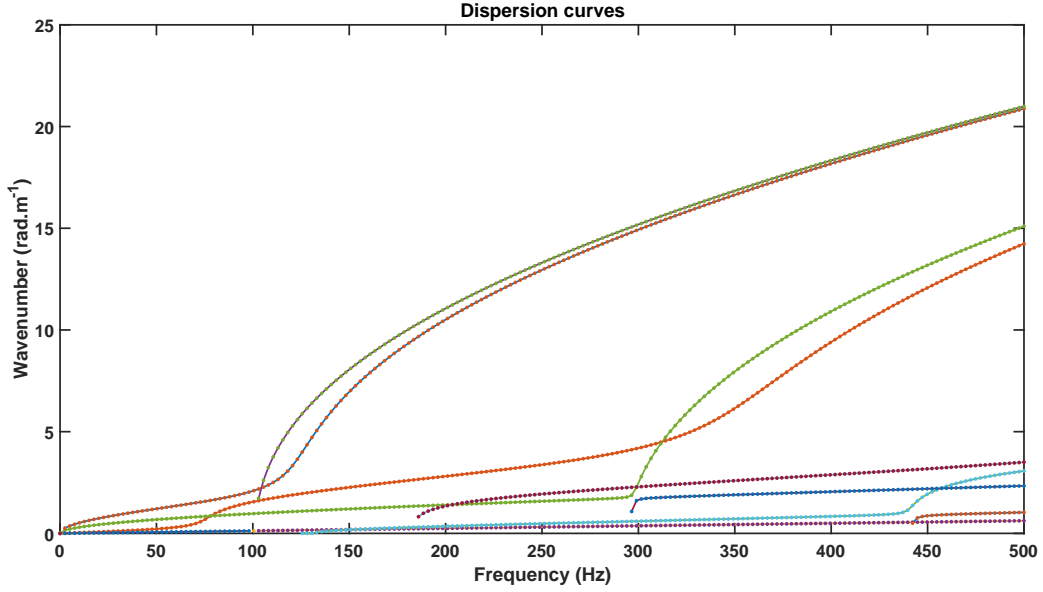


Figure 3: Dispersion curves of the hollow beam computed with the standard WFEM (.) and the reduced formulation (*). The two solutions are perfectly superposed.

Step	Reduced Model	Full Model	Reduction ratio
Model size	108	1440	13
Building reduced model	38.69s	NA	NA
WFE (per frequency)	$1.939 \cdot 10^{-2}$ s	28.02 s	1444
Total (200 frequencies)	42.58s	1h 34min	132

Table 1: Computational efforts required for the dispersion analyses in the hollow beam. Comparison between the reduced and full models. All calculations are conducted using an Intel(R) Core(TM) i7-6600U CPU 2.60GHz processor.

The relative error on the real and imaginary part are evaluated separately. Indeed, the the imaginary parts of wavenumbers of propagating waves are several orders of magnitude below that of the real parts but still contain important information about the wave propagation dynamics of the structure. Noteworthy, the error introduced by the reduction process is always inferior to 10^{-5} for the real part and the spikes appearing close to the cut-on frequencies are due to near zeros wavenumbers. The imaginary part is not as accurate at low frequency but stays below 10^{-5} after 40Hz, again, this is because the imaginary wavenumber is near 0 for propagative waves at 0 Hz. Therefore, it can be emphasized that the level of accuracy obtained with the reduced model is comparable to the level of precision of the eigenvalue solver, which mean that the error introduced by the reduction process is virtually null.

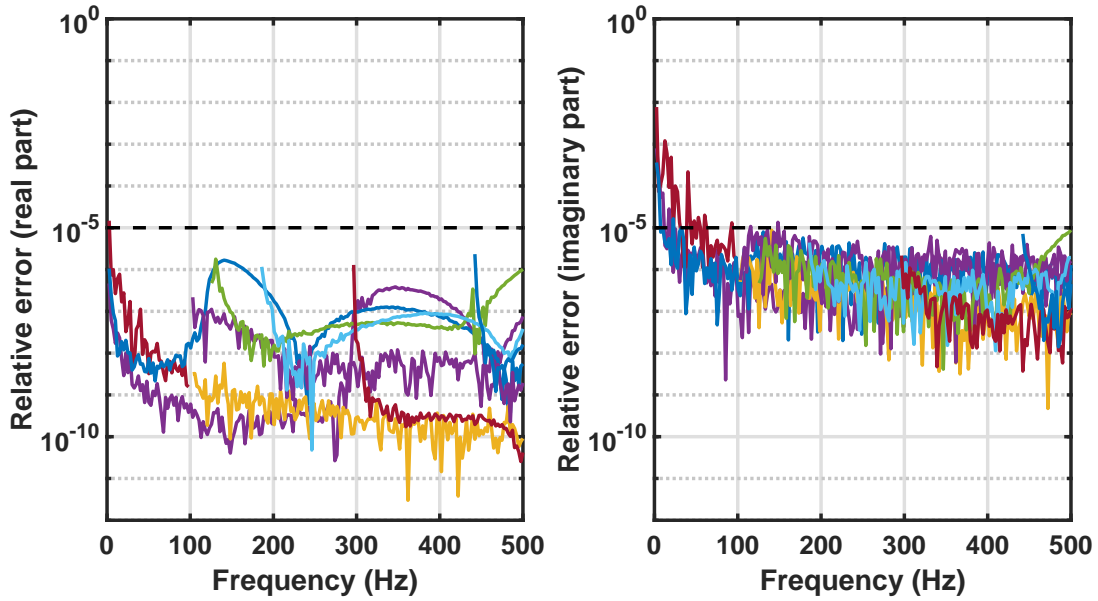


Figure 4: Error produced by the model order reduction scheme on the 9 propagating waves.

4.3. Performance of the method on a forced response framework

The ROM strategy is now applied to compute the dynamic response of the 12 m long finite structure. The forced response is obtained from the wave basis computed above, using the WFE forced response framework (see Mencik [18]). The beam is clamped on its left end (see Figure 5.a), while a punctual vertical load is applied on the right end, located on the center of the upper face, as shown in Figure 5.b.

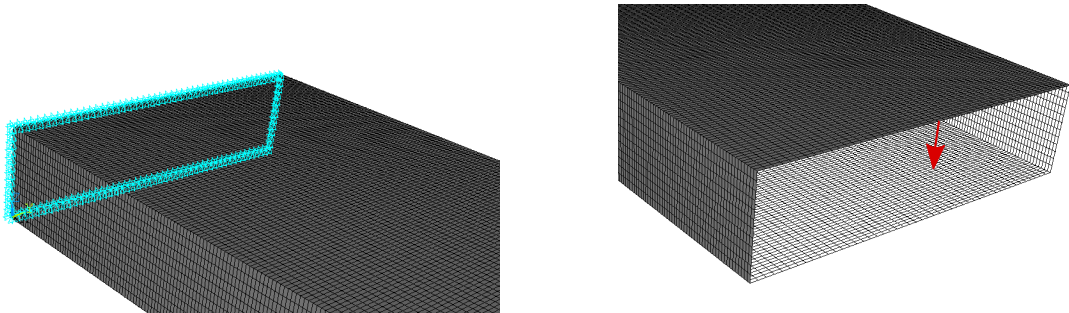


Figure 5: Boundary conditions and load applied to the hollow beam. The Left side of the beam is clamped while its right end is free. A unitary punctual force is applied at the middle of the cross section of the structure.

The forced response is computed in the same bandwidth [0 - 500 Hz], while the FE model described above is used to describe the waveguide's unit-cell. It is noted that the use of a Bloch formulation already provides significant advantages, since a similar simulation using standard FE analysis would result in a 2.16 millions DOF model. In order

to examine the convergence of the reduced model, 3 values of n_f are tested from $n_f=1$ to a $n_f=3$, while $n_k=3$ and ϵ is fixed to a conservative 10^{-5} (see Section 3.3). Results obtained from these three reduced models are compared with the full WFEM solution in Figure 6 (on point force excitation) and in Figure 7 (on the same cross-sectional location, at a 3 m distance from the excitation).

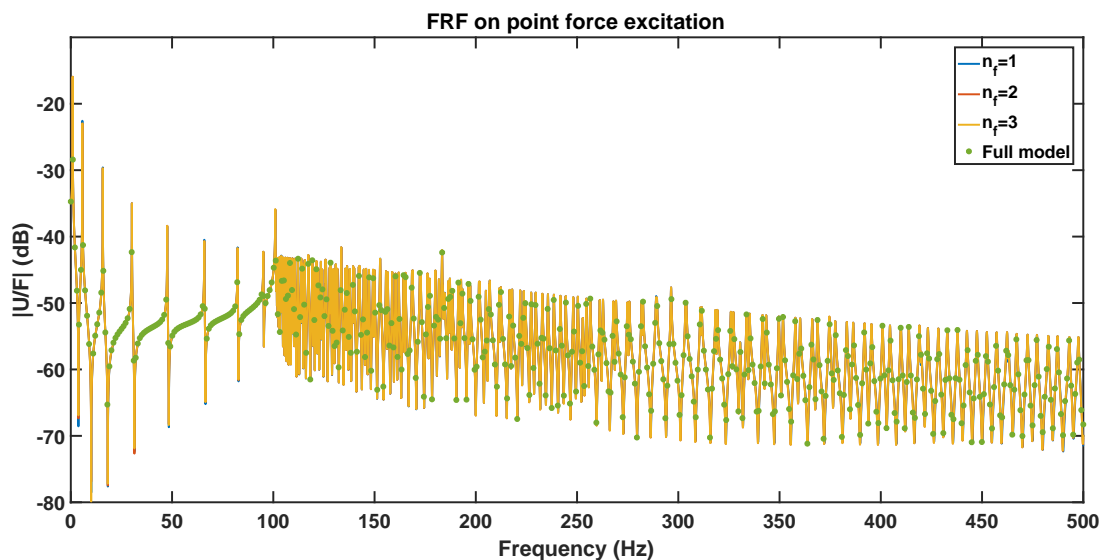


Figure 6: Forced response at the point force excitation. Proposed ROM ($n_f=1,2,3$) vs. full WFE model.

Noteworthy, the reduced model provides highly accurate frequency responses in both cases, as no error can be observed and convergence is already obtained for $n_f=1$. It means that the reduced model remains valid close to the singularity (on force point and boundary condition), and on the far field (second point). It is emphasized that such results would not be obtained if an insufficient number of waveshapes are retained. In a case where the far field is accurate but errors appear close to singularities, it is recommended to increase the value of n_f to 2 or 3.

Options	Reduced Model	Full Model	Reduction Factor
number of DOF	158	1440	9
Reduction process(time)	39.98s	NA	NA
WFE (time per frequency)	$5.00 \cdot 10^{-2}$ s	28.02s s	560
WFE (Total)	1m 40s ($2 \cdot 10^4$ frequencies)	3h 43m (500 frequencies)	NA
Forced Response	16m 40s ($2 \cdot 10^4$ frequencies)	10m 45s (500 frequencies)	NA
Total time	19m ($2 \cdot 10^4$ frequencies)	3h 54m (500 frequencies)	NA

Table 2: Computational efforts required for the forced response computation in the hollow beam. Comparison between the reduced ($n_f=3$, $n_k=3$, $\epsilon=10^{-5}$) and full models. All calculations are conducted using an Intel(R) Core(TM) i7-6600U CPU 2.60GHz processor.

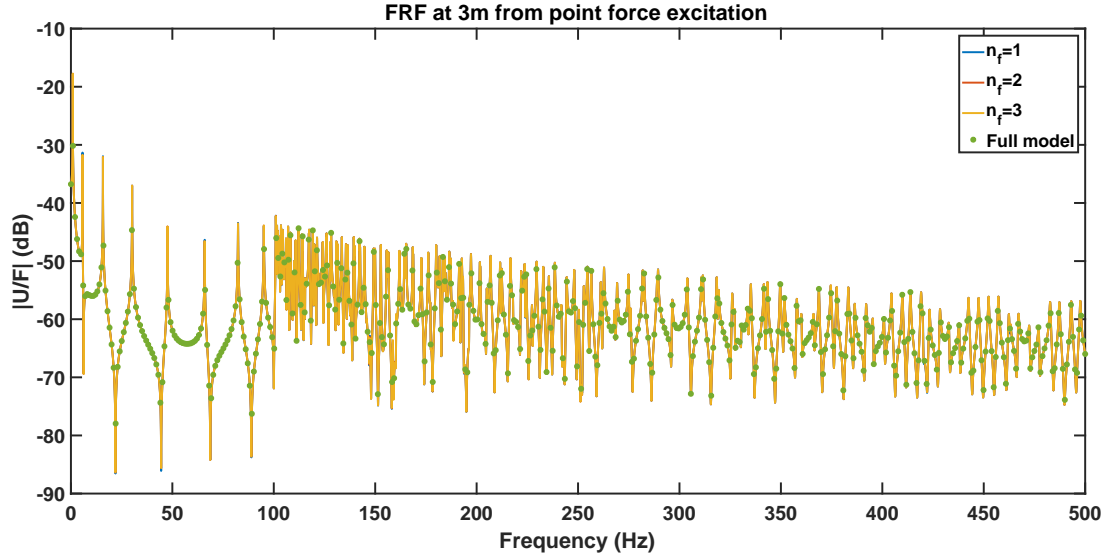


Figure 7: Forced response at 3 meters away from the point force excitation. Proposed ROM ($n_f=1,2,3$) vs. full WFE model.

The dynamic response of the hollow beam exhibits a clear transition from low- to mid-frequency behaviours, where the modal density increases drastically above 100 Hz. It is worth mentioning that this transition is produced by the cut-on and veering effects observed at the same frequency on the dispersion curves (Figure 3). In order to describe the dynamic behaviour of this waveguide, a high frequency resolution is required above 100 Hz, that would not be achievable using conventional FE methods nor standard forced WFEM formulation. A resolution of 20.000 frequency samples was possible using the reduced model (for a total of 19 min), while a similar WFEM computation would have required approximatively 160 hours. A detail of the computations realized is shown in Table 2. It compares the CPU time required to compute the FRF using the most conservative (largest model) case $n_f=3$ with the full model. When computing forced responses, the authors recommend to use a truncation criteria of $n_f=3$ to ensure convergence of the response at the point of excitation, while a value of $n_f=1$ or 2 is sufficient for accurate far field computations.

5. Validation 2: application to a stiffened plate

In this second validation example the method is applied to an orthogonally stiffened panel, which therefore combines periodicity in the propagation direction with a higher cross-sectional complexity. The application of the Bloch theorem via a direct approach is particularly challenging in such structures, as the number of DOF becomes larger and Component Mode Synthesis (CMS) is needed to perform dynamic condensation of the periodic unit-cell. This application example is proposed to highlight the performances of the proposed reduction scheme in a context where Bragg scattering and locally resonant behaviours are encountered within the acoustic range. Some sub-wavelength propagation features occurring in the mid-frequencies are further discussed, as it is emphasized that such high-resolution

dispersion analyses are hardly achievable from existing WFEM formulations.

5.1. Description of the stiffened structure

The considered waveguide is an aluminium plate of thickness $e=2$ mm and width 40 cm stiffened using rectangular beams of height $h=10$ mm and width $l_s=5$ mm. The spacing between the stiffeners is 10 cm along the width and 5 cm along the propagation direction and hysteretic damping of $\eta=10^{-4}$ is introduced. The FE model of a periodic unit-cell of the structure is shown in Figure 8. In order to allow fast dynamic condensation of the dynamic stiffness matrices, 31 fixed-interface modes are retained (until $10\times$ the maximum frequency) in the CMS, to replace the inner DOF of the periodic unit-cell. Then, the proposed wave-based reduction scheme is applied to further reduce the model on its interfaces.

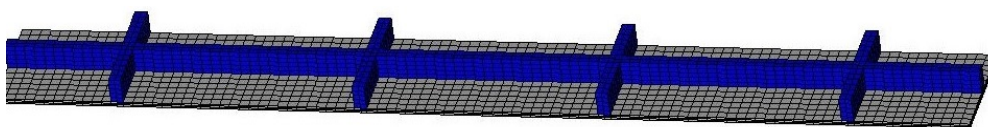


Figure 8: Unit-cell FE model of the orthogonally stiffened panel. Linear SOLID185 ANSYS elements are employed to mesh the whole structure, three elements are used in the plate's thickness and 10 elements are used to describe the stiffeners' cross-sections. A total of 26.331 DOF are used, while 2.880 DOF are located on the left and right interfaces of the periodic-cell.

5.2. Results and discussion of propagative behaviours in stiffened plates

The dispersion curves were obtained using the standard WFEM formulation (201 frequency samples, 10 h computation) and using the proposed method (5001 frequency samples, 9 min total computation). A summary of the CPU effort for each step is detailed in Table 3 for both reduced and full WFEM dispersion analyses.

Step	Proposed method (time)	WFEM + CMS (time)	Reduction Factor
Model size	194	2902	15
Craig-Bampton Reduction	2m 29s	2m 29s	NA
Wave-based reduction	3m 40s	NA	NA
WFE (per freq.)	4.21×10^{-2}s	3m 02s	4323
WFE (Total)	3m 30s (5001 freq.)	10h 09m (201 freq.)	NA
Total time	9m 40s (5001 freq.)	10h 11m (201 freq.)	NA

Table 3: Computation times for dispersion analysis in the stiffened structure. Comparison between the reduced ($n_f=3$, $n_k=3$, $\epsilon=10^{-5}$) and full models. All calculations are conducted using an Intel(R) Core(TM) i7-6600U CPU 2.60GHz processor.

Noteworthy, the model size is reduced by a factor 15 and yields almost negligible computational effort per frequency, while results are in perfect agreement with the full model (see Figure 9). Noteworthy, all dispersion effects

such as resonances, cut-on, veering and locking effects produced by backscattering waves are correctly described by the reduced model. The propagating dispersion curves of the waveguide are filtered using the criteria $|\lambda| > 0.9$ and a wavematching algorithm is used to identify wavetypes in the frequency range [0 - 5000 Hz]. Note that wavematching algorithms are highly sensitive to the frequency resolution. Therefore, the benefit of a refined frequency sampling becomes clearly visible between [4500 - 5000 Hz], where numerous veering-locking effects are observed in the dispersion curves.

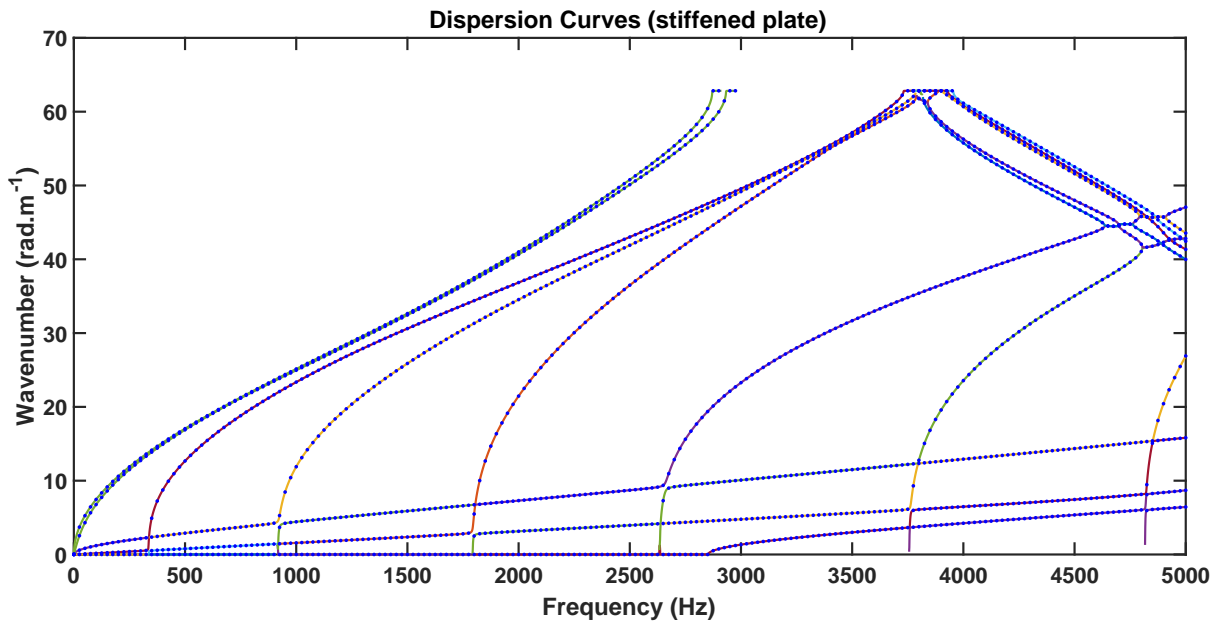


Figure 9: Dispersion curves of the stiffened plate, obtained using the standard WFEM (. . .) and the proposed reduction scheme (—) (both include CMS condensation).

Bragg scattering is also correctly predicted using the reduced model, and can be observed on first-order waves starting from 2900 Hz (for $k=62.83 \text{ rad.m}^{-1}$), note that the first local resonances occur in the same bandwidth in this example. In total, 11 propagating waves can be distinguished on the dispersion curves. The shapes of the first-order waves (longitudinal, shear, torsional and flexural) are shown in Figures 10 and 11 for a propagation along 0.5 m. Note that the plate behaves as an homogeneous structure in the considered bandwidth, as the wavelength is smaller than the stiffener's spacing in both propagating and transverse directions.

Cut-on frequencies of the out-of-plane waves are visible at 342 Hz, 925 Hz, 1800 Hz, 2633 Hz, 3757 Hz and 4817 Hz, and an additional cut-on is observed for in-plane motion at 2850 Hz. The deformed shapes of flexural waves' unit cells, computed close to their cut-on frequency are shown in Figures 12, 13 and 14. In the case of 1D propagation in waveguides with finite cross-section, these waves are also called guided resonances and propagate along the direction (Y) while exhibiting a finite wavelength in the transverse direction (X). It should be mentioned

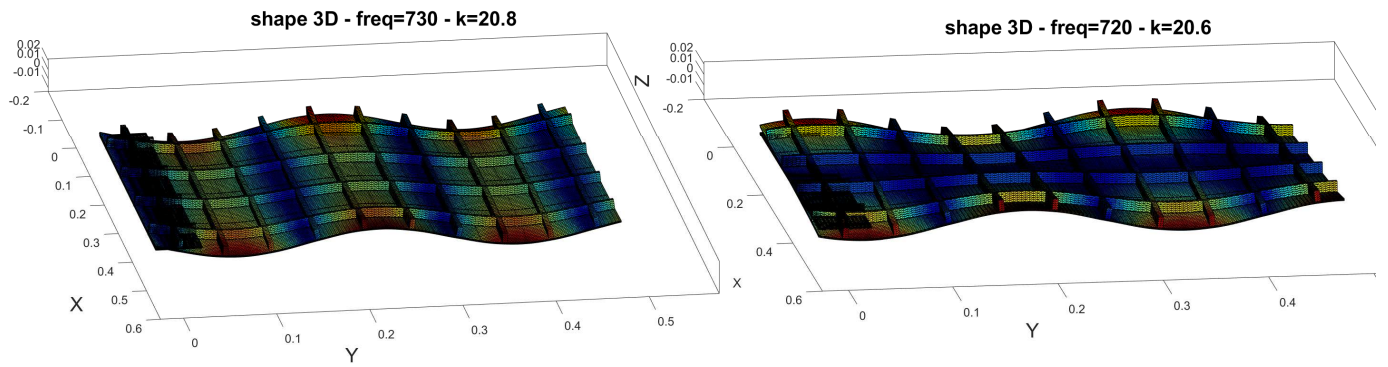


Figure 10: Flexural wave shape (left). Torsional wave shape (right). A normalized colormap is used to describe overall displacement amplitude.

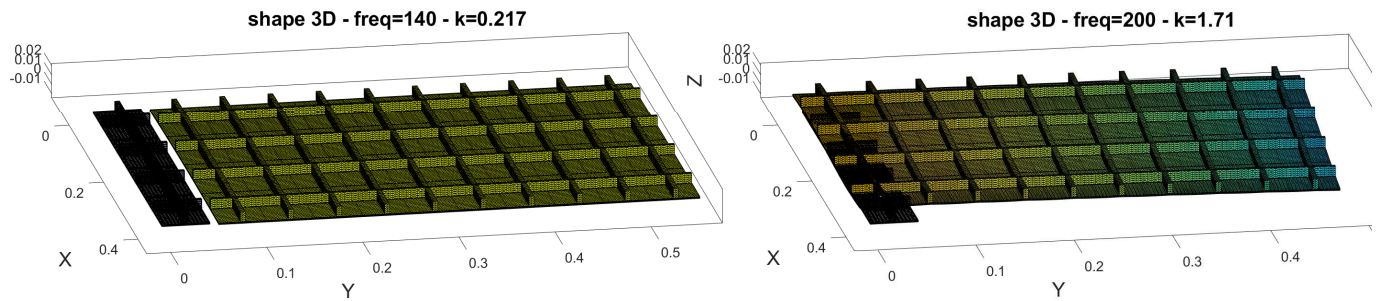


Figure 11: Longitudinal wave shape (left). Shear wave shape (right). A normalized colormap is used to describe overall displacement amplitude.

that these waves are usually dispersive close to their cut-on frequency, as their group velocity is close to 0.

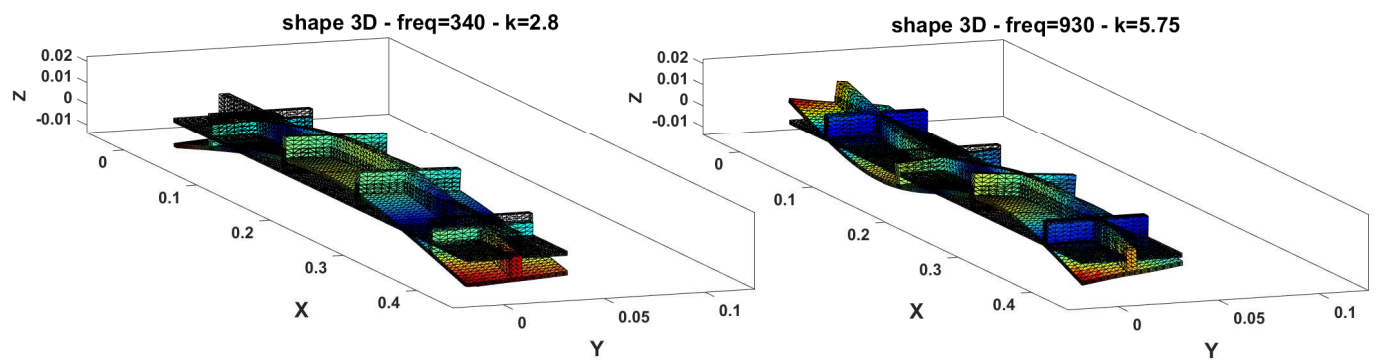


Figure 12: Deformed shapes of the periodic unit-cell close to the cut-on frequencies (2nd (a) and 3rd-order (b))

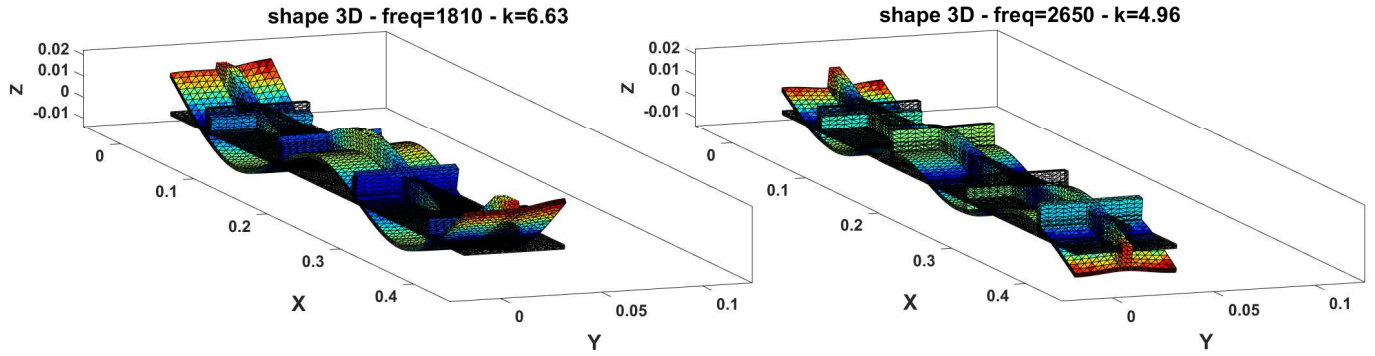


Figure 13: Deformed shapes of the periodic unit-cell close to the cut-on frequencies (4th (a) and 5th-order (b))

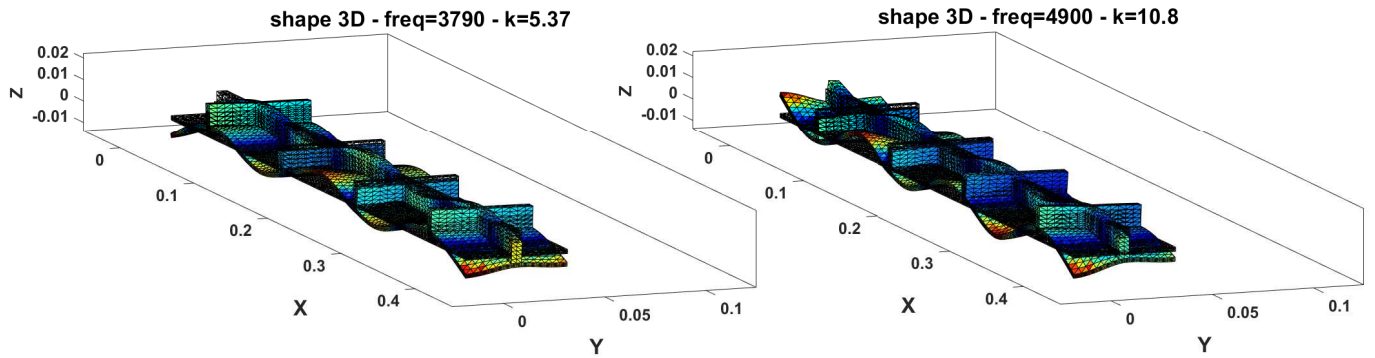


Figure 14: Deformed shapes of the periodic unit-cell close to the cut-on frequencies (5th (a) and 6th-order (b))

5.3. Waveguiding along stiffeners

The waves shown above are all guided by the free edges of the structure. Therefore, any modification of the boundary conditions would result in different dispersion properties, while a local excitation (as used in 4) is expected to generate multiple guided resonances. However, the 4th-order wave (cut-on at 1800 Hz) as the particularity of exhibiting a transverse wavelength comparable to the stiffeners' transverse spacing. This creates the possibility of a singular propagation feature, where a bandgap is present in the X direction, while propagation can occur in the main (Y) direction. Such behaviours can be observed at 3470 Hz and 4010 Hz. The propagation along 10 unit-cells (0.5 m) is shown in Figures 15 and 16. At these frequencies, uni-directional propagation can be obtained due to the longitudinal stiffeners.

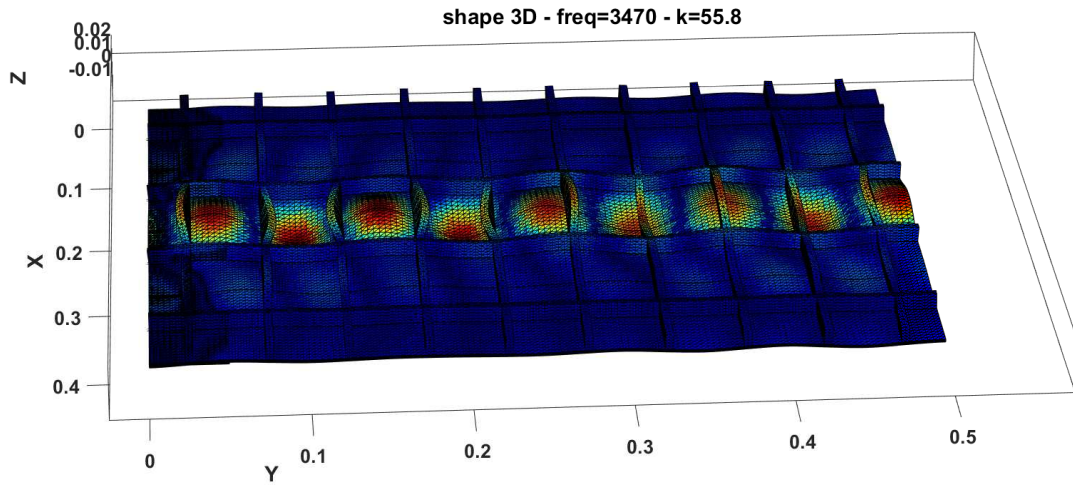


Figure 15: Propagation of a guided wave at 3470 Hz along a 0.5 m-long waveguide.

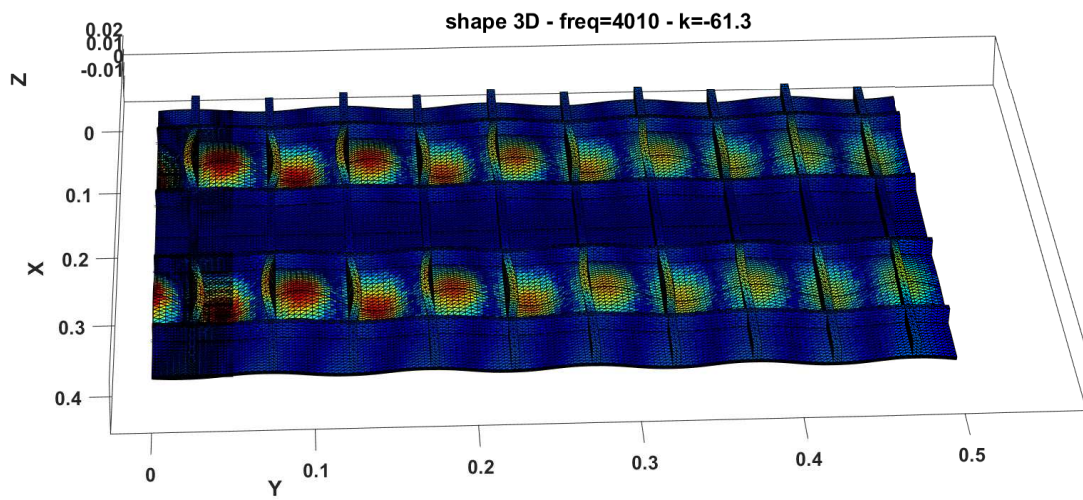


Figure 16: Propagation of a guided wave at 4010 Hz along a 0.5 m-long waveguide.

6. Conclusion

This paper presents a model order reduction strategy for the Wave Finite Element (WFE) Framework. The reduction scheme is based on the computation of a small number of inverse Bloch problems, while a single direct Bloch computation is required to evaluate the k -space sampling values. It is emphasized that an iterative eigenvalue solver should be used to benefit from reduced computational efforts both in the inverse Bloch problems and in the Component

Mode Synthesis when periodic structures are considered. Since these eigenvalue problems are well-conditioned, the creation of a reduced model can be performed on large models. The collection of eigenvectors obtained at k -samples is then processed through a Singular Value Decomposition and truncated to build the reduced wave basis, which can then be used in a direct (frequency-dependent) approach.

The reduction factor obtained is considerable (above 1000), taking into account the CMS and the reduction process. In comparison, it is emphasized that the other direct Bloch-based reduction techniques available in the literature [18, 19] usually provide one order of magnitude reduction of the computational effort. It should also be mentioned that the error is negligible in the proposed method (below 10^{-5} , almost the eigenvalue solver precision). This enables dynamic response analysis of finite structures with high accuracy, even when a large number of unit-cells is considered (3000 periods are used in the example of Sec. 4).

Additionally, since the contributions of the evanescent waves are still present in the reduced model it is possible to describe the displacement field close to singular loads and complex boundary conditions, or to study waves' interactions near a coupling element between two waveguides. Eventually, as the method provides a fast direct computation of the band diagrams, it is hoped that this will help encompass the current numerical limitations of FE-based cellular structure optimization exploiting Bragg or local resonance stop-band effects. The application to metamaterial design optimization will be the subject of forthcoming research.

Acknowledgements

The research of R. Boukadia was funded by an Early Stage Researcher grant within the European Project VIPER Marie Curie European Joint Doctorates (GA 675441). The research of C. Droz was funded by SIM (Strategic Initiative Materials in Flanders) and VLAIO (Flanders Innovation & Entrepreneurship) in the framework of the project DEMOPRECI, which is part of the research program MADUROS. The Research Fund KU Leuven is gratefully acknowledged for its support. This research was partially supported by Flanders Make, the strategic research centre for the manufacturing industry.

References

- [1] Liu, M., Xiang, J., Zhong, Y.. The band gap and transmission characteristics investigation of local resonant quaternary phononic crystals with periodic coating. *Applied Acoustics* 2015;100:10 – 17.
- [2] Collet, M., Fan, Y., Ichchou, M.. Periodically distributed piezoelectric patches optimization for waves attenuation and vibrations damping. *The Journal of the Acoustical Society of America* 2015;138(3):1920–1920.
- [3] Ruzzene, M., Scarpa, F., Soranna, F.. Wave beaming effects in two-dimensional cellular structures. *Smart materials and structures* 2003;12(3):363.
- [4] Ruzzene, M., Scarpa, F.. Control of wave propagation in sandwich beams with auxetic core. *Journal of intelligent material systems and structures* 2003;14(7):443–453.
- [5] Antonakakis, T., Craster, R., Guenneau, S.. High-frequency homogenization of zero-frequency stop band photonic and phononic crystals. *New Journal of Physics* 2013;15(10):103014.

- [6] Boutin, C., Becot, F.X.. Theory and experiments on poro-acoustics with inner resonators. *Wave Motion* 2015;54:76 – 99.
- [7] Casadei, F., Rimoli, J., Ruzzene, M.. A geometric multiscale finite element method for the dynamic analysis of heterogeneous solids. *Computer Methods in Applied Mechanics and Engineering* 2013;263:56–70.
- [8] Hussein, M.I., Hulbert, G.M.. Mode-enriched dispersion models of periodic materials within a multiscale mixed finite element framework. *Finite elements in analysis and design* 2006;42(7):602–612.
- [9] Zergoune, Z., Ichchou, M., Bareille, O., Harras, B., Benamar, R., Troclet, B.. Assessments of shear core effects on sound transmission loss through sandwich panels using a two-scale approach. *Computers & Structures* 2017;182:227–237.
- [10] Droz, C., Zergoune, Z., Boukadia, R., Bareille, O., Ichchou, M.. Vibro-acoustic optimisation of sandwich panels using the wave/finite element method. *Composite Structures* 2016;156:108–114.
- [11] Serra, Q., Ichchou, M., Deü, J.F.. Wave properties in poroelastic media using a wave finite element method. *Journal of Sound and Vibration* 2015;335:125–146.
- [12] Bhuddi, A., Gobert, M.L., Mencik, J.M.. On the acoustic radiation of axisymmetric fluid-filled pipes using the wave finite element (wfe) method. *Journal of Computational Acoustics* 2015;23(03):1550011.
- [13] Parrinello, A., Ghiringhelli, G.. Transfer matrix representation for periodic planar media. *Journal of Sound and Vibration* 2016;371:196–209.
- [14] Christen, J.L., Ichchou, M., Zine, A., Troclet, B.. Wave finite element formulation of the acoustic transmission through complex infinite plates. *Acta Acustica united with Acustica* 2016;102(6):984–991.
- [15] Waki, Y., Mace, B., Brennan, M.. Numerical issues concerning the wave and finite element method for free and forced vibrations of waveguides. *Journal of Sound and Vibration* 2009;327(1):92 – 108.
- [16] Claeys, C.C., Sas, P., Desmet, W.. On the acoustic radiation efficiency of local resonance based stop band materials. *Journal of Sound and Vibration* 2014;333(14):3203 – 3213.
- [17] Kook, J., Jensen, J.S.. Topology optimization of periodic microstructures for enhanced loss factor using acoustic-structure interaction. *International Journal of Solids and Structures* 2017;122-123:59–68.
- [18] Mencik, J.M.. A model reduction strategy for computing the forced response of elastic waveguides using the wave finite element method. *Computer Methods in Applied Mechanics and Engineering* 2012;229:68–86.
- [19] Mencik, J.M., Duhamel, D.. A wave-based model reduction technique for the description of the dynamic behavior of periodic structures involving arbitrary-shaped substructures and large-sized finite element models. *Finite Elements in Analysis and Design* 2015;101:1 – 14.
- [20] Zhou, C., Lainé, J.P., Ichchou, M.N., Zine, A.M.. Multi-scale modelling for two-dimensional periodic structures using a combined mode/wave based approach. *Computers & Structures* 2015;154:145 – 162.
- [21] Droz, C., Lainé, J.P., Ichchou, M., Inquiétude, G.. A reduced formulation for the free-wave propagation analysis in composite structures. *Composite Structures* 2014;113:134 – 144.
- [22] Droz, C., Zhou, C., Ichchou, M.N., Lainé, J.P.. A hybrid wave-mode formulation for the vibro-acoustic analysis of 2d periodic structures. *Journal of Sound and Vibration* 2016;363:285 – 302.
- [23] Mead, D.. A general theory of harmonic wave propagation in linear periodic systems with multiple coupling. *Journal of Sound and Vibration* 1973;27(2):235 – 260.
- [24] Mead, D.J.. The forced vibration of one-dimensional multi-coupled periodic structures: An application to finite element analysis. *Journal of Sound and Vibration* 2009;319(1):282 – 304.
- [25] Collet, M., Cunefare, K.A., Ichchou, M.N.. Wave motion optimization in periodically distributed shunted piezocomposite beam structures. *Journal of Intelligent Material Systems and Structures* 2009;20(7):787–808.
- [26] Waki, Y., Mace, B., Brennan, M.. Free and forced vibrations of a tyre using a wave/finite element approach. *Journal of Sound and Vibration* 2009;323(3):737 – 756.
- [27] Zhou, W., Ichchou, M.. Wave propagation in mechanical waveguide with curved members using wave finite element solution. *Computer Methods in Applied Mechanics and Engineering* 2010;199(33):2099 – 2109.
- [28] Zhong, W., Williams, F.. On the direct solution of wave propagation for repetitive structures. *Journal of Sound and Vibration* 1995;181(3):485

– 501.

- [29] Roy, O., Vetterli, M.. The effective rank: A measure of effective dimensionality. In: Signal Processing Conference, 2007 15th European. IEEE; 2007, p. 606–610.